Creation of a persistent current and vortex in a Bose-Einstein condensate of alkali-metal atoms

Tomoya Isoshima,* Mikio Nakahara,[1,2] Tetsuo Ohmi,[1,3] and Kazushige Machida[1]
[1]*Department of Physics, Okayama University, Okayama 700-8530, Japan*
[2]*Department of Physics, Kinki University, Higashi-Osaka 577-8502, Japan*
[3]*Department of Physics, Graduate School of Science, Kyoto University, Kyoto 606-8502, Japan*
(Received 1 September 1999; published 16 May 2000)

It is shown theoretically that a persistent current can be continuously created in a Bose-Einstein condensate (BEC) of alkali-metal atoms confined in a multiply connected region by making use of a spin degree of freedom of the order parameter of a BEC. We demonstrate that this persistent current is easily transformed into a vortex. Relaxation processes of these BEC after the confining field is turned off are also studied, so that our analyses are compared with time-of-flight experiments. The results are shown to clearly reflect the existence of a persistent current.

PACS number(s): 03.75.Fi, 67.40.Vs, 05.30.Jp

I. INTRODUCTION

Since the discovery of Bose-Einstein condensation in alkali-metal atoms [1], numerous attempts are made to show that the system exhibits superfluidity. One of these attempts is to create and observe quantized vortices. Recently the vortex is indeed created [2] using a two-component Bose-Einstein condensate (BEC).

In the present paper, we propose a method to create a state with a persistent current or a vortex, where the hyperfine spin F of alkali-metal atoms is fully utilized. This method was briefly reported on in Ref. [3], and more detailed theoretical and numerical analyses are made in the present paper. Although we restrict ourselves mainly to the case $F=1$ to simplify our discussions, our method is also applicable to cases with an arbitrary F.

A BEC with $F=1$ may be expressed in terms of a three-component order parameter, similarly to the spin or the orbital part of superfluid ^{3}He. In particular, a spin-polarized BEC has the same order parameter as that of ^{3}He-A [4]. In the case where the spin-exchange interaction is ferromagnetic, the BEC is spin polarized even in the absence of an external magnetic field. Even when the spin-exchange interaction is antiferromagnetic, it may also be spin polarized, provided that the Zeeman energy is larger than the spin-exchange energy. Accordingly, each of the weak-field-seeking states and strong-field-seeking states has the same order parameter as in ^{3}He-A.

In contrast with ^{3}He-A, the local order parameter configuration, known as a *texture* in ^{3}He [4], of a spin-polarized BEC may be easily controllable by a magnetic field. Making use of this property, a BEC in a vortex state or with a persistent current can be continuously created from a BEC without circulation by adiabatically changing an external magnetic field, as shown below. Quite recently topological manipulation of a BEC with internal degrees of freedom was realized experimentally by utilizing that freedom [5].

The general theoretical framework for describing a spinor BEC [6] was given by Ohmi and Machida [7], and independently by Ho [8], whose calculations turned out to be equivalent. This framework is based on the Bogoliubov theory extended to a vectorial order parameter with three components, corresponding to $m_F=1$, 0, and -1 of the $F=1$ atomic hyperfine state. As a result, the generalized Gross-Pitaevskii equation was constructed. They calculated low-lying collective modes such as sound waves, spin waves, and their coupled modes, and predicted various topological defects or spin textures.

This paper is organized as follows. In Sec. I, the order parameter of a BEC with $F=1$ is discussed. We employ two sets of basis vectors, and their transformations are also considered. Then the generalized Gross-Pitaevskii equation is introduced. In Sec. III, we consider the cross disgyration texture which is expected to appear in an Ioffe-Pritchard trap. Section IV is the main part of the present paper. We first consider an axially symmetric BEC without a current confined in an Ioffe-Pritchard trap with an optical plug. A strong magnetic field is applied along the axis of the BEC. Then the sign of this axial magnetic field is adiabatically changed so that the local magnetization vector flips in the end of this process. Then it is shown that a persistent current with two units of circulation is created. If the optical plug may be turned off at this stage, we are left with a vortex line. The topological justification for this behavior is also given. Observational consequences of the existence of a quantized vortex or a persistent current are discussed in Sec. V, where the relaxation of the order parameter after the confining fields are turned off is studied. Section VI is devoted to a summary and discussions.

II. SPINOR BOSE-EINSTEIN CONDENSATE

A. Spinor order parameter

Let F_α $(\alpha=x,y,z)$ be the angular momentum operators with $F=1$. The eigenvalues of F_z are 1, 0, and -1, and their corresponding eigenvectors, that satisfy $F_z|i\rangle=i|i\rangle$, are

$$|1\rangle=\begin{pmatrix}1\\0\\0\end{pmatrix},\qquad |0\rangle=\begin{pmatrix}0\\1\\0\end{pmatrix},\qquad |-1\rangle=\begin{pmatrix}0\\0\\1\end{pmatrix}. \tag{1}$$

*Electronic address: tomoya@mp.okayama-u.ac.jp

In this basis, called the z-quantized basis, F_α is represented as

$$F_x=\frac{1}{\sqrt{2}}\begin{pmatrix}0&1&0\\1&0&1\\0&1&0\end{pmatrix},$$

$$F_y=\frac{i}{\sqrt{2}}\begin{pmatrix}0&-1&0\\1&0&-1\\0&1&0\end{pmatrix}, \tag{2}$$

$$F_z=\begin{pmatrix}1&0&0\\0&0&0\\0&0&-1\end{pmatrix},$$

which satisfy the commutation relation $[F_\alpha,F_\beta]=iF_\gamma\varepsilon_{\alpha\beta\gamma}$. The order parameter $|\Psi\rangle$ is expanded in terms of $|i\rangle$ as

$$|\Psi\rangle=\sum_{i=0,\pm1}\Psi_i|i\rangle. \tag{3}$$

It is convenient for our purposes to introduce another set of basis vectors $|\alpha\rangle$ $(\alpha=x,y,z)$ called the XYZ basis which satisfy $F_\alpha|\alpha\rangle=0$. Note that $|z\rangle=|0\rangle$ by definition. The vectors $|x\rangle$ and $|y\rangle$ are obtained by rotating $|z\rangle$ around the y axis and the x axis by $\pm\pi/2$:

$$|x\rangle=\exp\left(-i\frac{\pi}{2}F_y\right)|z\rangle=\frac{1}{\sqrt{2}}(-|1\rangle+|-1\rangle), \tag{4}$$

$$|y\rangle=\exp\left(i\frac{\pi}{2}F_x\right)|z\rangle=\frac{i}{\sqrt{2}}(|1\rangle+|-1\rangle). \tag{5}$$

Then the order parameter $|\Psi\rangle$ may be decomposed in terms of $|\alpha\rangle$ as

$$|\Psi\rangle=\sum_{\alpha=x,y,z}\Psi_\alpha|\alpha\rangle. \tag{6}$$

The components Ψ_i and Ψ_α are related to each other as

$$\begin{pmatrix}\Psi_1\\\Psi_0\\\Psi_{-1}\end{pmatrix}=\begin{pmatrix}\frac{-1}{\sqrt{2}}&\frac{i}{\sqrt{2}}&0\\0&0&1\\\frac{1}{\sqrt{2}}&\frac{i}{\sqrt{2}}&0\end{pmatrix}\begin{pmatrix}\Psi_x\\\Psi_y\\\Psi_z\end{pmatrix}. \tag{7}$$

In a spin-polarized BEC, the weak- or strong-field-seeking state is represented by an order parameter

$$\mathbf{\Psi}=\frac{\psi}{\sqrt{2}}e^{i\alpha}(\hat{\boldsymbol{m}}+i\hat{\boldsymbol{n}}) \tag{8}$$

in the XYZ basis, where $\psi=\sqrt{\Sigma_k|\Psi_k|^2}$ and $\hat{\boldsymbol{m}}$ and $\hat{\boldsymbol{n}}$ are real unit vectors. We also define

$$\hat{\boldsymbol{l}}=\hat{\boldsymbol{m}}\times\hat{\boldsymbol{n}}, \tag{9}$$

which represents the direction of the atomic hyperspin. The three real vectors $(\hat{\boldsymbol{m}},\hat{\boldsymbol{n}},\hat{\boldsymbol{l}})$ form a triad.

In the above explanation the direction of the axis of quantization is named z. We may take this direction to be arbitrary. When the axis is parallel to the direction of the magnetic field (B in this paper), the Zeeman energy term is written most simply. We call this B-quantized (BQ) notation. When the direction of the axis does not vary spatially and parallel to the z axis, we call this z-quantized (ZQ) notation. The kinetic-energy term is written simply in this way. The numerical details are given in the Appendix.

B. Gross-Pitaevskii equations

The time-dependent form of the Gross-Pitaevskii (GP) equation with a spin-degree of freedom obtained by Ohmi and Machida [7], originally in the XYZ basis, can be rewritten in ZQ notation as

$$i\frac{\partial}{\partial t}\Psi_j=\Big\{h_{jk}+g_n\delta_{jk}\sum_l|\Psi_l|^2+g_s\sum_\alpha\sum_{lp}(\Psi_l(F_\alpha)_{lp}\Psi_p)(F_\alpha)_{jk}\Big\}\Psi_k, \tag{10}$$

where

$$h_{jk}(\mathbf{r})=\left(-\frac{\hbar^2\nabla^2}{2m}-\mu+V(\mathbf{r})\right)\delta_{jk}-\mathcal{B}_{jk}, \tag{11}$$

$$\mathcal{B}=\begin{pmatrix}B_z&\frac{B_x-iB_y}{\sqrt{2}}&0\\\frac{B_x+iB_y}{\sqrt{2}}&0&\frac{B_x-iB_y}{\sqrt{2}}\\0&\frac{B_x+iB_y}{\sqrt{2}}&-B_z\end{pmatrix}. \tag{12}$$

m is the mass of an atom, and $\boldsymbol{B}=(B_x,B_y,B_z)$ is a magnetic field scaled so that the amplitude is the Zeeman energy of the atom. The potential $V(\mathbf{r})$ is spin independent, and $i,j=0,\pm1$ are the spin indices in the ZQ basis. The parameters g_n and g_s denote the strength of the interactions. The relationship between (B_x,B_y,B_z) and $\mathcal{B}$ is explained in the Appendix. Time-independent solutions of GP equation are obtained by solving

$$0=\Big\{h_{jk}+g_n\delta_{jk}\sum_l|\Psi_l|^2+g_s\sum_\alpha\sum_{lp}(\Psi_l(F_\alpha)_{lp}\Psi_p)(F_\alpha)_{jk}\Big\}\Psi_k. \tag{13}$$

The above equations are derived from the Hamiltonian

$$H=\int d\boldsymbol{r}\sum_{jk}\Psi_j^\dagger(\boldsymbol{r})h_{jk}(\boldsymbol{r})\Psi_k(\boldsymbol{r}) + \frac{g_n}{2}\sum_{jk}\Psi_j^\dagger(\boldsymbol{r})\Psi_k^\dagger(\boldsymbol{r})\Psi_k(\boldsymbol{r})\Psi_j(\boldsymbol{r}) + \frac{g_s}{2}\sum_{\alpha}\left(\sum_{jk}\Psi_j^\dagger(\boldsymbol{r})(F_\alpha)_{jk}\Psi_k(\boldsymbol{r})\right)^2. \tag{14}$$

III. STRONG- AND WEAK-FIELD-SEEKING STATES IN AN IOFFE-PRITCHARD TRAP

We consider a system of BEC which is uniform along the z axis. The cylindrical coordinates $\boldsymbol{r}=(r,\phi,z)$ are introduced. Suppose that an Ioffe-Pritchard field

$$\boldsymbol{B}=(B_\perp(r)\cos\phi,-B_\perp(r)\sin\phi,B_z) \tag{15}$$

is applied to the system. We consider a two dimensional system of a BEC, uniform along the z axis, in the following calculations. So B_z is treated as a constant, which differs from the usual Ioffe-Pritchard field. There should be a blue-detuned laser beam penetrating along the z axis to prevent the atoms from escaping from the trap by spin flipping. Ohmi and Machida [7] showed that there appears the cross disgyration when $B_z=0$.

Let us derive the configuration of the condensate in this system. The $\mathcal{B}$ matrix [Eq. (12)] becomes

$$B=\begin{pmatrix} B_z & B_\perp\frac{e^{i\phi}}{\sqrt{2}} & 0 \\ B_\perp\frac{e^{-i\phi}}{\sqrt{2}} & 0 & B_\perp\frac{e^{i\phi}}{\sqrt{2}} \\ 0 & B_\perp\frac{e^{-i\phi}}{\sqrt{2}} & -B_z \end{pmatrix}. \tag{16}$$

The eigenvalues of $\mathcal{B}$ are $\pm B$ and 0, where $B=\sqrt{B_\perp^2+B_z^2}$, and the corresponding eigenvectors, denoted by $|i\rangle_{\mathrm{BQ}}$, are

$$|\pm1\rangle_{\mathrm{BQ}}=\frac{1}{2B}\begin{pmatrix}(B\pm B_z)e^{i\phi}\\ \pm\sqrt{2}B_\perp\\ (B\mp B_z)e^{-i\phi}\end{pmatrix}, \tag{17}$$

$$|0\rangle_{\mathrm{BQ}}=\frac{1}{\sqrt{2}B}\begin{pmatrix}-B_\perp e^{i\phi}\\ \sqrt{2}B_z\\ B_\perp e^{-i\phi}\end{pmatrix}. \tag{18}$$

The vectors $|1\rangle_{\mathrm{BQ}}$ and $|-1\rangle_{\mathrm{BQ}}$ are identified with the strong-field-seeking state and the weak-field-seeking state respectively. Accordingly when the whole system is in the strong- or the weak-field-seeking state, the order parameter is written in terms of these vectors as $|\Psi\rangle=\Psi(\boldsymbol{r})|\pm1\rangle_{\mathrm{BQ}}$. The $\mathcal{B}\Psi$ term in Eqs. (10) and (11) is then simplified to $\pm B(r)\Psi$, so that the GP equation takes the form

$$i\frac{\partial\Psi}{\partial t}=\left\{-\frac{\hbar^2\nabla^2}{2m}-\mu+V(r)\mp B(r)+(g_n+g_s)|\Psi|^2\right\}\Psi. \tag{19}$$

We have ignored the small corrections, which come from the spatial dependence of the quantization axis, to the kinetic-energy term. This is the usual GP equation without the spin degrees of freedom.

When $B_z=0$, the order parameter with the highest eigenvalue, corresponding to the strong-field-seeking state, is

$$\begin{pmatrix}\Psi_1\\ \Psi_0\\ \Psi_{-1}\end{pmatrix}=\psi\begin{pmatrix}\frac{1}{2}e^{i\phi}\\ \frac{1}{\sqrt{2}}\\ \frac{1}{2}e^{-i\phi}\end{pmatrix}e^{iw\phi}, \tag{20}$$

where w is an integer and ψ is the amplitude of $\boldsymbol{\Psi}$. In the XYZ basis, this is rewritten as

$$\begin{pmatrix}\Psi_x\\ \Psi_y\\ \Psi_z\end{pmatrix}=\psi\begin{pmatrix}-i\frac{1}{\sqrt{2}}\sin\phi\\ -i\frac{1}{\sqrt{2}}\cos\phi\\ \frac{1}{\sqrt{2}}\end{pmatrix}e^{iw\phi}. \tag{21}$$

The corresponding $\hat{\boldsymbol{m}}$, $\hat{\boldsymbol{n}}$, and $\hat{\boldsymbol{l}}$ vectors are

$$\hat{\boldsymbol{m}}=(\sin\phi\sin(w\phi),\cos\phi\sin(w\phi),\cos(w\phi)),$$
$$\hat{\boldsymbol{n}}=(-\sin\phi\cos(w\phi),-\cos\phi\cos(w\phi),\sin(w\phi)), \tag{22}$$
$$\hat{\boldsymbol{l}}=(\cos\phi,-\sin\phi,0).$$

In the weak-field-seeking state, the order parameter is written as

$$\begin{pmatrix}\Psi_1\\ \Psi_0\\ \Psi_{-1}\end{pmatrix}=\psi\begin{pmatrix}\frac{1}{2}e^{i\phi}\\ -\frac{1}{\sqrt{2}}\\ \frac{1}{2}e^{-i\phi}\end{pmatrix}e^{iw\phi} \tag{23}$$

or

$$\begin{pmatrix} \Psi_x \\ \Psi_y \\ \Psi_z \end{pmatrix} = \psi \begin{pmatrix} -i\frac{1}{\sqrt{2}}\sin\phi \\ -i\frac{1}{\sqrt{2}}\cos\phi \\ -\frac{1}{\sqrt{2}} \end{pmatrix} e^{iw\phi}. \tag{24}$$

The corresponding triad is

$$\hat{\boldsymbol{m}} = (\sin\phi\sin(w\phi), \cos\phi\sin(w\phi), -\cos(w\phi)),$$

$$\hat{\boldsymbol{n}} = (-\sin\phi\cos(w\phi), -\cos\phi\cos(w\phi), -\sin(w\phi)), \tag{25}$$

$$\hat{\boldsymbol{l}} = (-\cos\phi, \sin\phi, 0).$$

This $\hat{\boldsymbol{l}}$ vector field in both Eqs. (22) and (25) clearly represents the cross disgyration.

IV. CREATION OF VORTEX

In the present section, we propose a simple method to create a persistent current (and also a vortex state) in a torus-shaped BEC from a state with no persistent current. Then it will be shown that this persistent current is easily transformed to a vortex.

In the following we consider two cases separately. In case I, the condensate is confined optically and the spin of each atom points the direction of the magnetic field. That is, the atoms are strong-field seekers. In case II, the magnetic field is also used to confine the condensate. The spin of atoms points are antiparallel to the magnetic field, and the atoms are weak-field seekers. The former case has an advantage in its theoretical simplicity. On the other hand, the latter case does not require an apparatus for optical confinement except for the repulsive plug around $r=0$, and can be realizable more easily.

In the following discussions we consider a BEC of Na atoms with $F=1$. The mass of the atom $m=3.81\times10^{-26}$ kg, the interaction parameter is $g_n=4\pi\hbar^2 a/m$, and a scattering length $a=2.75\times10^{-9}$ m is employed. We ignore the other interaction parameter g_s. This is possible since the whole condensate is assumed to be in either a strong- or weak-field-seeking state as a whole in the following. In those states the interaction terms in the GP equation are reduced as shown in Eq. (19).

The particle density is taken to be around 10^{19} m^{-3}, and the detailed density profile is given in each figure. The time span of the persistent current creation process $T=30$ ms is chosen, since this is between (the Larmor frequency)$^{-1}$ ~1 m sec and the lifetime of the condensate ~1 sec.

A. Case I: optical confinement

The external magnetic field $\boldsymbol{B}(r,\phi,z)$ takes the form

$$(B_x, B_y) = B_\perp(\cos\phi, -\sin\phi),$$

$$B_z = B_{z0}\cos[\pi(1-t/T)], \tag{26}$$

$$B_\perp = B'_\perp r\sin[\pi(1-t/T)],$$

where t is the time. The factors of the field are taken to be $B'_\perp/h=200$ J/(h μm) and $B_{z0}/h=2\times10^3$ J/h (note that the scaled magnetic field represents the Zeeman energy and h is the Planck constant). One finds from Eq. (26) that B_z flips from $-B_{z0}$ to B_{z0}, so that $\hat{\boldsymbol{l}}$ also flips in the end of the evolution. The Larmor frequency is $\omega_L\sim0.6\times10^3$ Hz for $B/h\sim2\times10^3$ J/h. Thus $\omega_L T\sim18$. The spin-independent potential is

$$V(r) = \frac{m(2\pi\nu)^2}{2}r^2 + U\exp\left(-\frac{r^2}{2r_0^2}\right), \tag{27}$$

with $\nu=200$ Hz, $U/h=1\times10^4$ J/h and $r_0=5$ μm. The first term of Eq. (27) is the confining potential, while the second term is the potential produced by the optical plug.

We obtained the order parameter profile by numerical integration of the time-dependent GP equation (10). The initial state is taken to be the ground state with no circulation. The magnetic field changes the direction slowly from upward to downward according to Eq. (26), as shown in Fig. 1(a), so that the atoms remain in the strong-field-seeking state. The change in the number of the kth component,

$$N_k(t) = \int |\Psi_k(\mathbf{r},t)|^2 d^2\mathbf{r} \quad (k=-1,0,1) \tag{28}$$

is shown in Fig. 1(b). The total particle density

$$n(r,t) = \sum_k |\Psi_k(r,t)|^2 \tag{29}$$

changes with the magnetic field, as shown in Fig. 1(c).

The resulting triad configurations are shown in Fig. 2 for $t=0$, 15, and 30 ms. Figure 2(a) shows the initial vector configurations. Figure 2(b) shows the vector configurations when $t=15$ ms. The $\hat{\boldsymbol{l}}$ texture is nothing but the cross disgyration explained in Sec. III since B_z now vanishes. We see that the vectors $\hat{\boldsymbol{m}}$ and $\hat{\boldsymbol{n}}$ rotate around $\hat{\boldsymbol{l}}$ by 2π as we go around the z axis once. Finally when $t=30$ ms, we obtain a texture with $\hat{\boldsymbol{l}}$ almost points up everywhere. The vectors $\hat{\boldsymbol{m}}$ and $\hat{\boldsymbol{n}}$ rotate around $\hat{\boldsymbol{l}}$ by 4π as one goes around the z axis once in this case, and one finally obtains a uniform $\hat{\boldsymbol{l}}$ texture with a circulation with a winding number 2.

Now that a persistent current is created, it is easy to transform this into a vortex. The BEC has a $k=1$ component only at $t=30$ ms. Then there are no atoms near the axis $r=0$ since the centrifugal force prevents the atoms from coming close to the axis. Thus one may simply turn off the optical plug to obtain a vortex. The details are analyzed in Sec. IV B.

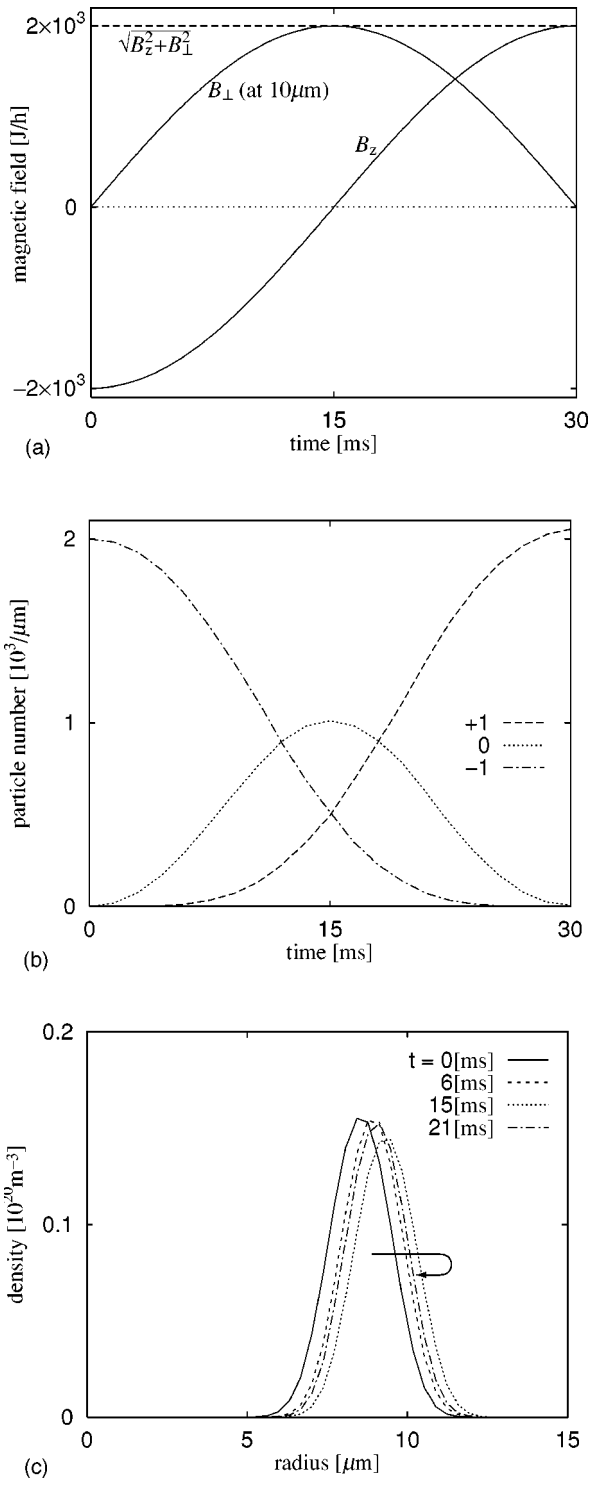

FIG. 1. The process of the persistent current creation in case I. (a) Magnetic field at $r=10\ \mu$m as a function of time. Because $B_\perp \propto r$, the total magnetic field varies slightly at $r \neq 10\ \mu$m. (b) Particle numbers N_k as a function of time. The condensate has a Ψ_{-1} component only at $t=0$, and a Ψ_1 component only at $t=T$. (c) Total number density distribution. The condensate is almost fixed at around $r=9\ \mu$m by the optical potential $V(r)$. However, the change of the total magnetic field [see caption (a)] causes the change in the radial distribution, as shown here.

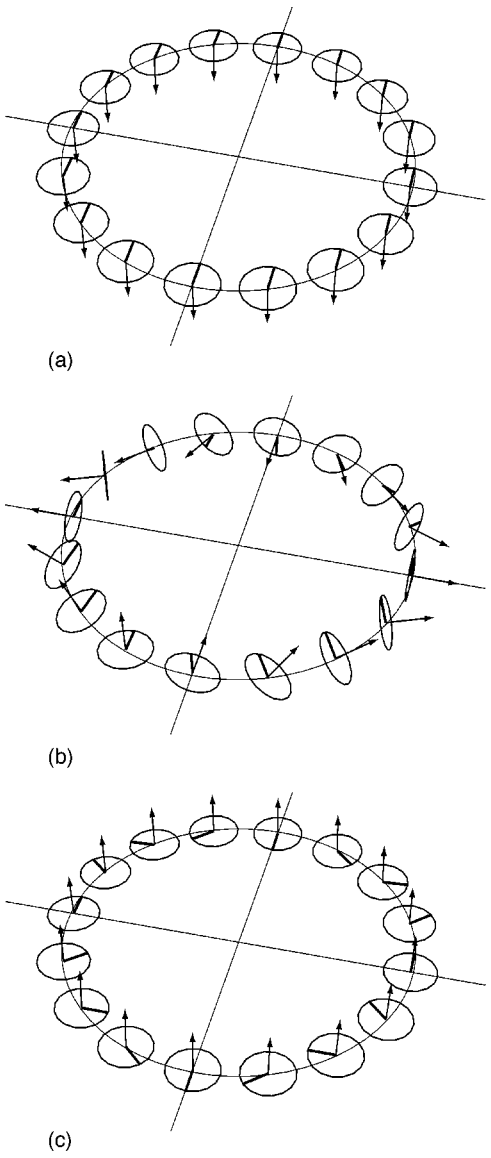

FIG. 2. The triad configurations for $t=0$, 15, and 30 ms. The arrows denote $\hat{\boldsymbol{l}}$, while $\hat{\boldsymbol{m}}$ and $\hat{\boldsymbol{n}}$ are on the disk. The line on the disk is $\hat{\boldsymbol{m}}$. Note that there is no need to draw $\hat{\boldsymbol{n}}$ since it is uniquely given by $\hat{\boldsymbol{l}}\times\hat{\boldsymbol{m}}$. When $t=0$ and 30 ms, $\hat{\boldsymbol{l}}$ points down and up, respectively. When $t=15$ ms, $\hat{\boldsymbol{l}}$ lies almost on the xy plane.

B. Case II: magnetic confinement

In case I, the condensate is confined with a spin-independent optical trap. Here in case II, we consider a situation where the quadrapole magnetic field [Eq. (15)] always exists, and the additional field B_z changes from a large positive value to a large negative value as shown in Fig. 3(a):

$$(B_x, B_y) = B_\perp(\cos\phi, -\sin\phi),$$

$$B_z = B_{z0}(1-2t/T), \tag{30}$$

$$B_\perp = B'_\perp r.$$

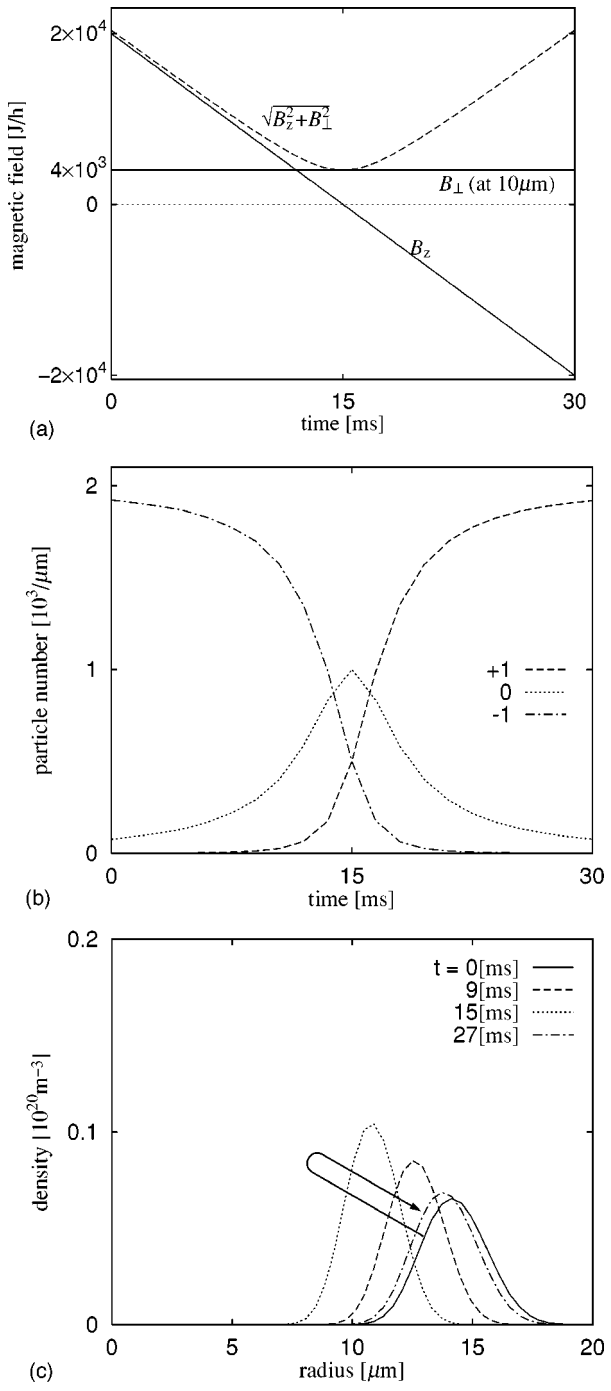

FIG. 3. The process of persistent current creation in case II. (a) Magnetic field at $r=10\ \mu$m as a function of time. Initially B_z is positive, in contrast with case I. (b) Particle numbers N_k as functions of time. The condensate is mostly composed of a Ψ_{-1} component at $t=0$, while and mostly of a Ψ_1 component at $t=T$. (c) Total density distribution. Contrary to case I, the condensate is confined by the $B_\perp$ part of the magnetic field at larger r. Then the radial change is more eminent than that of case I.

Here we take $B'_\perp/h=400$ J/(h μm), $B_{z0}/h=2\times10^4$ J/h, and $T=30$ ms. Contrary to case I, the atoms are in a weak-field-seeking state, and the gradient of B_r is responsible for the confinement of the condensate. The optical plug produces a spin-independent potential

$$V(r)=U\exp\left(-\frac{r^2}{2r_0^2}\right), \tag{31}$$

where we take $U/h=1\times10^4$ J/h and $r_0=5$ μm.

The evolution of the order parameter field was analyzed numerically, and it was found that the order parameter configurations in this case are essentially the same as in case I. Figure 3(b) shows the temporal evolution of the components $N_k(t)$, and Fig. 3(c) shows the total density profile at various times.

The persistent current created here may also be transformed into a vortex. The BEC is mostly composed of a $k=1$ component at $t=30$ ms, and there is only a small number of atoms near $r=0$. Suppose the optical plug is turned off. Then atoms will escape but this process should be very slow. Thus one expects that the vortex is stable for a considerable period of time.

C. Mathematical analysis of continuous creation of circulation

It may be surprising that we have *continuously* created a persistent current (a vortex) from a system without circulation. Mathematically this is justified by invoking homotopy theory [9,10]. Let us denote a rotation around direction $\hat{\boldsymbol{n}}$ by an angle α by a ''vector'' $\alpha\hat{\boldsymbol{e}}$. This rotation is expressed as a rotation matrix

$$R(\hat{\boldsymbol{e}},\alpha)=(1-\cos\alpha)\hat{n}_i\hat{n}_j+\cos\alpha\,\delta_{ij}-\sin\alpha\,\varepsilon_{ijk}\hat{n}_k. \tag{32}$$

Since α may be restricted within the region $0\leqslant\alpha\leqslant\pi$, the set of all the rotations is represented by a ball B^3 with the radius π. Note however that the points $\pi\hat{\boldsymbol{e}}$ and $-\pi\hat{\boldsymbol{e}}$ corresponds to equivalent rotations. Thus all the antipodal points on the surface of the ball must be identified. This space B^3/Z_2 is called the three-dimensional real projective space, denoted by $\mathcal{P}^3$.

Let us take a ''standard'' triad $(\hat{\boldsymbol{m}}_0,\hat{\boldsymbol{n}}_0,\hat{\boldsymbol{l}}_0)$ shown in Fig. 4. Then an arbitrary triad is obtained by applying a certain rotation $\alpha\hat{\boldsymbol{e}}$ to the standard triad. Thus the local vector configuration is in one-to-one correspondence with a point in $\mathcal{P}^3$.

Consider an order parameter configuration shown in Fig. 2(a). When one circumnavigates the circle, one finds that all the triads along the circle are obtained from the standard one by applying no rotations, namely, $\alpha=0$. Thus this circle is mapped to the origin of $\mathcal{P}^3$. Next consider the triads in Fig. 2(b). As one goes along the circle, one finds that the standard triad is rotated by an angle $\pi/2$ around the axis $\hat{\boldsymbol{e}}=(-\sin\phi,-\cos\phi,0)$ shown in Fig. 4 Thus this circle is mapped to a circle in $\mathcal{P}^3$ with the radius $\pi/2$; see Fig. 4. Finally, consider the triads in Fig. 2(c). All the $\hat{\boldsymbol{l}}$ vectors point up, and the standard triad is rotated by π around the axis $\hat{\boldsymbol{e}}$ given above. Thus the the circle in Fig. 2(c) is mapped to a great circle with the radius π.

The change of the images in $\mathcal{P}^3$, namely, a point $\rightarrow$ a circle with the radius $\pi/2\rightarrow$ a circle with the radius π, is continuous (or more precisely homotopic), which shows that the deformation of the triads is indeed continuous. In con-

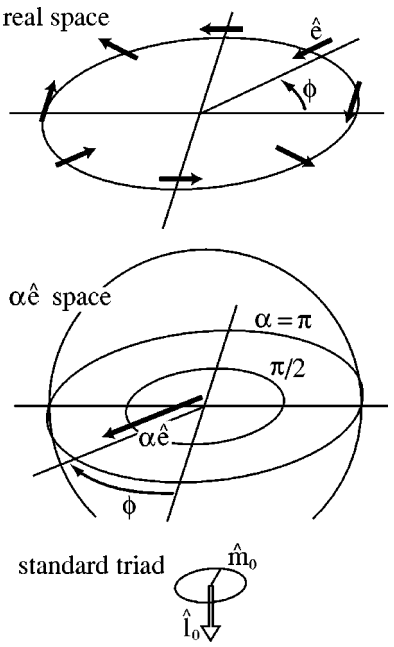

FIG. 4. The real-space configuration of $\hat{\mathbf{e}}$, the $\mathcal{P}^3$ space and the standard triad. The thick arrows are $\alpha\hat{\mathbf{e}}$ vectors.

figuration (a), the vector $\hat{\boldsymbol{m}}$ does not rotate around $\hat{\boldsymbol{l}}$ and therefore there is no current flowing around the circle. In configuration (b), however, $\hat{\boldsymbol{m}}$ rotates around $\hat{\boldsymbol{l}}$ while one goes along the circle once, which implies a vortex of winding number 1. Similarly, $\hat{\boldsymbol{m}}$ winds around $\hat{\boldsymbol{l}}$ twice in configuration (c), and the vortex has the winding number 2. We stress again that the creation of this winding number (or circulation) is continuous and the final configuration is stable so far as the external magnetic field forces $\hat{\boldsymbol{l}}$ to point upward.

D. Angular momentum analysis of current creation

The continuous current creation can be explained more generally using the eigenvectors of the $\mathcal{B}$ matrix with the highest and lowest eigenvalues in the BQ basis. The magnetic field expressed in the $\mathcal{B}$ matrix is the dominant factor that determines the behavior of the order parameter $\boldsymbol{\Psi}$. We first discuss a BEC with $F=1$, which we have analyzed in the present paper.

The magnetic fields [Eq. (26) in case I and Eq. (30) in case II] are of the form of Eq. (15). The corresponding $\mathcal{B}$ matrix is given by Eq. (16). Because the magnetic fields are sufficiently strong, we may assume that the order parameter $\boldsymbol{\Psi}$ is proportional to the highest (upper sign) or lowest (lower sign) eigenvector,

$$|\pm 1\rangle_{\mathrm{BQ}}=\frac{1}{2B}\begin{pmatrix}(B\pm B_z)e^{i\phi}\\ \pm\sqrt{2}B_\perp\\ (B\mp B_z)e^{-i\phi}\end{pmatrix}, \tag{33}$$

of the $\mathcal{B}$ matrix. Case I uses the highest (upper sign) eigenvector, and case II uses the lowest (lower sign) eigenvector. The order parameter is

$$\begin{pmatrix}\Psi_1\\ \Psi_0\\ \Psi_{-1}\end{pmatrix}=C\begin{pmatrix}(B\pm B_z)e^{i\phi}\\ \pm\sqrt{2}B_\perp\\ (B\mp B_z)e^{-i\phi}\end{pmatrix}e^{iw\phi}, \tag{34}$$

where C is a complex number independent of ϕ and w is an integer.

Let us consider case I (case II can be analyzed similarly). When $t=0$, the magnetic field is $(B_\perp,B_z)=(0,\mp B_{z0})$. As shown in Eq. (34), the condensate behaves as $\Psi_{-1}\propto e^{i(w-1)\phi}$ and $\Psi_0=\Psi_1=0$. Because we start with a state with no circulation, the integer w must be 1.

The components B_z and $B_\perp$ change as shown in, for example, Fig. 1(a), from $t=0$ to $t=T$. Both $B_\perp$ and $(B\pm B_z)$ have finite values during the change, and the condensate $\boldsymbol{\Psi}$ stays in the strong-field-seeking state. The phase factor w will not change during the process for the order parameter to be defined uniquely. Thus we take $w\equiv 1$ throughout the process. When $t=T$, the magnetic field is $(B_\perp,B_z)=(0,\pm B_{z0})$. Since $w=1$, Eq. (34) leads to the conclusion that we have a condensate with $\Psi_1\propto e^{2i\phi}$ and $\Psi_0=\Psi_{-1}=0$. Accordingly a vortex with the winding number 2 has been created.

A similar discussion is possible in the system with $F=2$ atoms using the eigenvector given in Eq. (A7). Starting from a state with no winding number, we eventually obtain a state with the winding number 4.

V. DETECTION OF VORTEX: TIME-OF-FLIGHT IMAGING

The detection of a vortex (or persistent current) has been a problem as difficult as their creation. We consider the relaxation of the spinor texture after the confining field and the optical plug are turned off to facilitate the comparison between our theory and experiments, in particular the time-of-flight analysis.

The temporal evolution of the BEC is described by the time-dependent GP equation (10). We consider case I and case II separately.

A. Case I

We consider three cases where the confining potentials are turned off separately at $t=0$, $T/2$, and T ms. There is no vortex at $t=0$, while there is a vortex with a winding number 2 at $t=T$. The comparison between these two cases is essential to observe our vortex.

(i) $t=0$: The condensate has a component Ψ_{-1} only. The density profile at $t=0$ is determined by solving the time-independent GP equation. The relaxation process after the potentials are turned off is found by solving the time-dependent GP equation (10), whose result is shown in Fig. 5(a). Since Ψ_{-1} has no singularity at the origin, the condensate fills the central region $(r\sim 0)$ in later time. It is interesting to note that the components Ψ_0 and Ψ_1 do not appear at a later time since the total spin must be conserved.

(ii) $t=T/2$: The cross disgyration appears in this stage. The order parameter of this texture is given by Eq. (20) with $w=1$. Thus all the components are nonvanishing in this case.

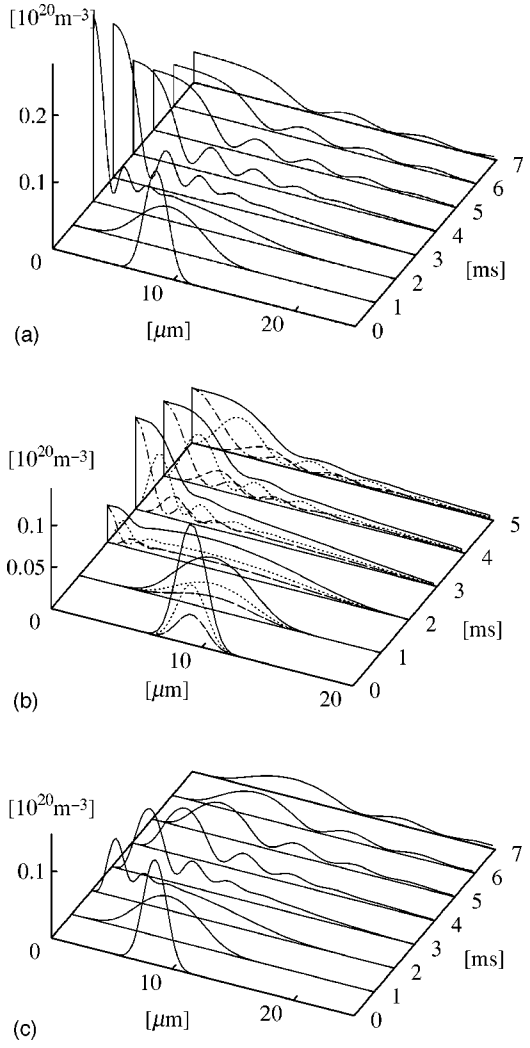

FIG. 5. Temporal evolution of the condensate. (a) The potentials are turned off at $t=0$. The solid line is the total density purely made of $|\Psi_{-1}|^2$. (b) The potentials are turned off at $t=T/2$. The solid line is the total density $\Sigma_k|\Psi_k|^2$ while the dashed line, the dotted line, and the dash-dotted line are components $|\Psi_1|^2$, $|\Psi_0|^2$, and $|\Psi_{-1}|^2$, respectively. The corresponding winding numbers are 2, 1, and 0. (c) The potentials are turned off at $t=T$. The solid line is the total number density, composed of $|\Psi_1|^2$ only. The condensate has the winding number 2 and cannot fill the central region. This should be compared with (a) and (b). The three axes are the density (10^{20} m^{-3}), the radial direction (μm), and time (ms).

After the potentials are turned off at $t=0$ the order parameter relaxes, as shown in Fig. 5(b). The component Ψ_0 has a winding number 1, while Ψ_1 has a winding number 2, and hence they cannot fill the central region. The central region near $r=0$ may be filled only with the Ψ_{-1} component, since it has vanishing winding number. Note also that the Ψ_0 component is dominant in the vicinity of $r\sim 1$ μm.

(iii) $t=T$: The vector $\hat{\boldsymbol{l}}$ points up now, and hence $\Psi_{-1}=\Psi_0=0$, while $\Psi_1\neq 0$. Figure 5(c) shows the temporal evolution of the order parameter after the potentials are turned off. Since the order parameter has a nontrivial phase factor, it cannot fill the central region at all in later times. Similarly to case (i), the components Ψ_0 and Ψ_{-1} do not appear in the relaxation process. The absence of the condensate at $r=0$ at an arbitrary time is a clear distinction between case (iii) and the rest, which may be used to show the existence of the vortex or the persistent current experimentally.

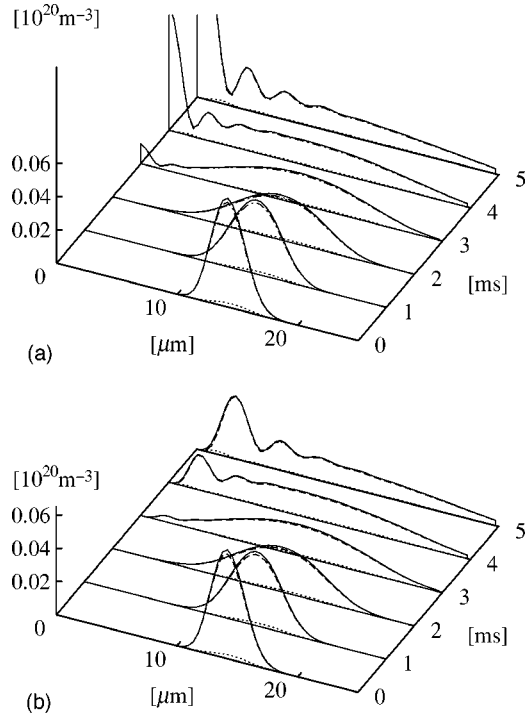

FIG. 6. Temporal evolution of the condensates when the potentials are turned off at (a) $t=0$ and (b) $t=T$. In both cases the description of the lines are the same as that in Fig. 5. The three axes are the density (10^{20} m^{-3}), the radial direction (μm), and time (ms).

Comparing Figs. 5(a), 5(b), and 5(c), we find the following: The empty region around $r=0$, which shows the existence of the vortex, has a length scale an order of 10 μm after 7-ms relaxation, and the length will be sufficient to observe experimentally. Because the length scale of the central vacuum region is almost the same as that of the density waves at larger r (outer), the resolution of the imaging will be checked by the outer density waves.

B. Case II

Figure 6(a) shows the relaxation process when the potentials are turned off at $t=0$, while they are turned off at $t=T$ in Fig. 6(b). Because the magnetic field is not exactly parallel or antiparallel to the z axis, the nondominant component of the condensate appears slightly in both cases.

VI. SUMMARY AND DISCUSSIONS

In summary, we have proposed a method to create a persistent current and a vortex with the winding number 2 in a Bose-Einstein condensate of alkali-metal atoms. The dynamics of vortex creation are simulated by solving the time-dependent Gross-Pitaevskii (GP) equation. The continuity of this process is justified by invoking homotopy theory and also by the angular momentum analysis. The existence of the

vortex may be demonstrated by comparing the time-of-flight data before and after the vortex creation.

It is also possible to create a persistent current or a vortex with the winding number 1. Suppose one prepares the ground state in the Ioffe-Pritchard field. The resulting texture is the cross disgyration with no winding of the $\hat{\boldsymbol{m}}$ vector around the $\hat{\boldsymbol{l}}$ vector as shown in [7]. Then apply a strong magnetic field B_z either parallel to or antiparallel to the z axis. The $\hat{\boldsymbol{l}}$ vector in the resulting texture points up or down, depending on the direction of B_z or whether the state is weak field seeking or strong field seeking. In any case, the $\hat{\boldsymbol{m}}$ vector rotates around $\hat{\boldsymbol{l}}$ once as one circumnavigates around the z axis once. Thus one obtains a persistent current or a vortex of the winding number 1 by simply preparing a sample in the Ioffe-Pritchard trap and applying a strong magnetic field along the z axis.

ACKNOWLEDGMENTS

The work of MN was supported partially by a Grant-in-Aid for Scientific Research Fund of the Ministry of Education, Science, Sports and Culture, No. 11640361.

APPENDIX: MAGNETIC-FIELD MATRIX

We consider a system of atoms with spin $F=f$. The F matrices, which are the angular momentum operators, are given by

$$F_x=\begin{pmatrix} 0 & \frac{\sqrt{2f\times 1}}{2} & & & \\ \frac{\sqrt{2f\times 1}}{2} & 0 & \frac{\sqrt{(2f-1)2}}{2} & & \\ & \frac{\sqrt{(2f-1)2}}{2} & \ddots & \ddots & \\ & & \ddots & 0 & \frac{\sqrt{1\times 2f}}{2} \\ & & & \frac{\sqrt{1\times 2f}}{2} & 0 \end{pmatrix},$$

$$F_y=\begin{pmatrix} 0 & \frac{\sqrt{2f\times 1}}{2i} & & & \\ -\frac{\sqrt{2f\times 1}}{2i} & 0 & \frac{\sqrt{(2f-1)2}}{2i} & & \\ & -\frac{\sqrt{(2f-1)2}}{2i} & \ddots & \ddots & \\ & & \ddots & 0 & \frac{\sqrt{1\times 2f}}{2i} \\ & & & -\frac{\sqrt{1\times 2f}}{2i} & 0 \end{pmatrix}, \tag{A1}$$

$$(F_z)_{jj}=f+1-j \quad (j=1,2,\ldots,2f+1).$$

They satisfy the commutation relation $[F_\alpha,F_\beta]=iF_\gamma\varepsilon_{\alpha\beta\gamma}$.

We write the magnetic field with a B vector

$$\begin{pmatrix} B_x \\ B_y \\ B_z \end{pmatrix}=B\begin{pmatrix} \sin\theta_y\cos\theta_z \\ \sin\theta_y\sin\theta_z \\ \cos\theta_y \end{pmatrix}=\begin{pmatrix} B_\perp\cos\theta_z \\ B_\perp\sin\theta_z \\ B_z \end{pmatrix}, \tag{A2}$$

where $0\leqslant\theta_y\leqslant\pi$ and $0\leqslant\theta_z<2\pi$. The amplitude $|\vec{B}|$ is scaled so that it represents the Zeeman energy.

The order parameter of a BEC is written with a vector of $2f+1$ components, and operators are expressed in terms of $(2f+1)\times(2f+1)$ square matrices. We call the operator for the Zeeman energy for $\mathcal{B}$ matrix. We can choose the quantization axis so that the $\mathcal{B}$ matrix is proportional to the matrix F_z. We call this the B-quantized (BQ) notation, because B is proportional to the quantization axis.

The $\mathcal{B}$ matrix in the ZQ notation is obtained by successive spatial rotations θ_y along the y axis and θ_z along the z axis, as

$$\mathcal{B}_{\mathrm{ZQ}}=U^{\dagger}\mathcal{B}_{\mathrm{BQ}}U, \tag{A3}$$

$$U^{\dagger}=\exp(-iF_z\theta_z)\exp(-iF_y\theta_y).$$

Let us study a few examples. When $f=1$,

$$\mathcal{B}_{\mathrm{ZQ}}=\begin{pmatrix} B_z & \frac{B_\perp}{\sqrt{2}}e^{-i\theta_z} & 0 \\ \frac{B_\perp}{\sqrt{2}}e^{i\theta_z} & 0 & \frac{B_\perp}{\sqrt{2}}e^{-i\theta_z} \\ 0 & \frac{B_\perp}{\sqrt{2}}e^{i\theta_z} & -B_z \end{pmatrix}. \tag{A4}$$

The eigenvector with the lowest eigenvalue is

$$U^{\dagger}\begin{pmatrix}0\\0\\1\end{pmatrix}=\begin{pmatrix} \frac{B-B_z}{2}e^{-i\theta_z} \\ -\frac{B_\perp}{\sqrt{2}} \\ \frac{B+B_z}{2}e^{i\theta_z} \end{pmatrix}. \tag{A5}$$

When $f=2$,

$$\mathcal{B}_{\mathrm{ZQ}}=\begin{pmatrix} 2B_z & B_\perp e^{-i\theta_z} & 0 & 0 & 0 \\ B_\perp e^{i\theta_z} & B_z & \sqrt{\frac{3}{2}}B_\perp e^{-i\theta_z} & 0 & 0 \\ 0 & \sqrt{\frac{3}{2}}B_\perp e^{i\theta_z} & 0 & \sqrt{\frac{3}{2}}B_\perp e^{-i\theta_z} & 0 \\ 0 & 0 & \sqrt{\frac{3}{2}}B_\perp e^{i\theta_z} & -B_z & B_\perp e^{-i\theta_z} \\ 0 & 0 & 0 & B_\perp e^{i\theta_z} & -2B_z \end{pmatrix}. \tag{A6}$$

The eigenvector with the lowest eigenvalue is

$$U^{\dagger}\begin{pmatrix}0\\0\\0\\0\\1\end{pmatrix}=C\begin{pmatrix} B\left(\frac{1-\cos\theta_y}{2}\right)^2 e^{-2i\theta_z} \\ -B\frac{\sin\theta_y}{2}(1-\cos\theta_y)e^{-i\theta_z} \\ B(\sin\theta_y)^2\sqrt{\frac{3}{8}} \\ -B\frac{\sin\theta_y}{2}(1+\cos\theta_y)e^{i\theta_z} \\ B\left(\frac{1+\cos\theta_y}{2}\right)^2 e^{2i\theta_z} \end{pmatrix}. \tag{A7}$$

[1] For a review, see F. Dalfovo, S. Giorgini, L. P. Pitaevskii, and S. Stringari, Rev. Mod. Phys. **71**, 463 (1999).

[2] M. R. Matthews, B. P. Andrson, P. C. Haljan, D. S. Hall, C. E. Wieman, and E. A. Cornell, Phys. Rev. Lett. **83**, 2498 (1999).

[3] M. Nakahara, T. Isoshima, K. Machida, S. Ogawa, and T. Ohmi, e-print, cond-mat/9905374.

[4] D. Vollhardt and P. Wölfle, *The Superfluid Phases of He 3* (Taylor & Francis, London, 1990).

[5] M. R. Matthews, B. P. Anderson, P. C. Haljan, D. S. Hall, M. J. Holland, J. E. Williams, C. E. Wieman, and E. A. Cornell, Phys. Rev. Lett. **83**, 3358 (1999).

[6] J. Stenger, S. Inouye, D. M. Stamper-Kurn, H.-J. Miesner, A. P. Chikkatur, and W. Ketterle, Nature (London) **396**, 345 (1998).

[7] T. Ohmi and K. Machida, J. Phys. Soc. Jpn. **67**, 1822 (1998).

[8] T.-L. Ho, Phys. Rev. Lett. **81**, 742 (1998).

[9] N. D. Mermin, Rev. Mod. Phys. **51**, 591 (1979).

[10] M. Nakahara, *Geometry, Topology and Physics* (Adam Hilger, Bristol, 1990).